Full Paper

Propellants, Explosives, Pyrotechnics

DOI: 10.1002/prep.201300187

Study on the Synthesis and Interfacial Interaction Performance of Novel Dodecylamine-Based Bonding Agents Used for Composite Solid Propellants

Yu Chen,*[a] Yun-fei Liu,[a] Liang Shi,[a] Wei Yang,[a] and Wei-shang Yao[a]

Abstract: An effective pathway was explored to design and select proper bonding agents that could effectively improve the interfacial interactions between bonding agents and solid particles, with three novel synthesized alkyl bonding agents, dodecylamine-*N*,*N*-di-2-hydroxypropyl-acetate (DIHPA), dodecylamine-*N*,*N*-di-2-hydroxypropyl-hydroxyacetate (DIHPHA) and dodecylamine-*N*,*N*-di-2-hydroxypropyl-cyano-acetate (DIHPCA), as examples. Molecular dynamics simulation was applied to compare unit bond energies of these bonding agents with the [110] crystal face of ammonium perchlorate (AP) and the [120] crystal face of hexogen (RDX). The infrared test was used to characterize the interfacial interactions of these bonding agents with AP or RDX. XPS test was applied to calculate the adhesion percentage of the bonding agents on the surface of precoated AP or RDX particles. All of the above results indicated that these three bonding agents have strong interfacial interactions with AP or RDX in the order of DIHPCA > DIHPHA > DIHPA. The prepared three bonding agents were used in HTPB/AP/RDX/Al propellants, and their effects on tensile strength (σ), elongation under maximum tensile strength (ε_m), elongation at breaking point of the propellant (ε_b) and adhesion index (Φ) of the propellant were studied. The results show that the bonding agents improve the mechanical properties of the propellant in the order of DIHPCA > DIHPHA > DIHPA. The methods found from theoretical design, materials synthesis, and mechanistics studies up to practical application show effective guiding significance for choosing the proper bonding agent and improving the interfacial interactions between the solid particles and binder matrix.

Keywords: Bonding agents · Interfacial interactions · Ammonium perchlorate · Hexogen · Composite solid propellants

1 Introduction

Composite solid propellants are a class of special particle-reinforced composites, which are commonly applied for the energy source of rockets or missiles. They are composed by the binder matrix and the solid packing, such as explosive, oxidant, metal fuel, etc. The solid mass content of the above solid packing is usually higher than 70%. The interfacial interactions between the binder matrix and the surface of nitramine explosives, ammonium perchlorate, as well as other solid filling particles have significant impact on the mechanical properties of composite solid propellants [1]. When an external force is exerted to the solid propellant, weak interfacial interactions between binder matrix and the solid filling particles may cause debonding of the solid particles and destruction of the propellant, resulting in holes in the stretched direction and inducing further crack damages for energetic propellants [2,3]. Pre-coating of solid particle surfaces [4,5] or the addition of bonding agents (also known as coupling agents) to the propellant formulations [6–8] is widely applied to improve the interfacial interactions between solid particles and binder matrix and ameliorate mechanical properties of the propellants. Bonding agents contain functional groups that can both interact with solid filling particles and react with the binder matrix. Thus, they are able to enhance the interfacial interactions between solid particles and binder matrix in composite solid propellants [9–12], and play an important role in improving mechanical properties of composite solid propellants. The commonly used bonding agents in composite solid propellants include aziridine and its derivatives, alkanolamine and its derivatives, polyamine and its derivatives, titanate compounds, hydantoin compounds, neutral polymeric bonding agents, among others [13–15].

However, the improving effects of bonding agents on the interfacial interactions are difficult to be studied, and there are only a few and imprecise methods to design and select proper bonding agents that could really improve the interfacial interactions between the solid filling particles and binder matrix.

[a] *Y. Chen, Y.-f. Liu, L. Shi, W. Yang, W.-s. Yao*
School of Materials Science and Engineering
Beijing Institute of Technology
Beijing 100081, P. R. China
**e-mail: cylsy@163.com*

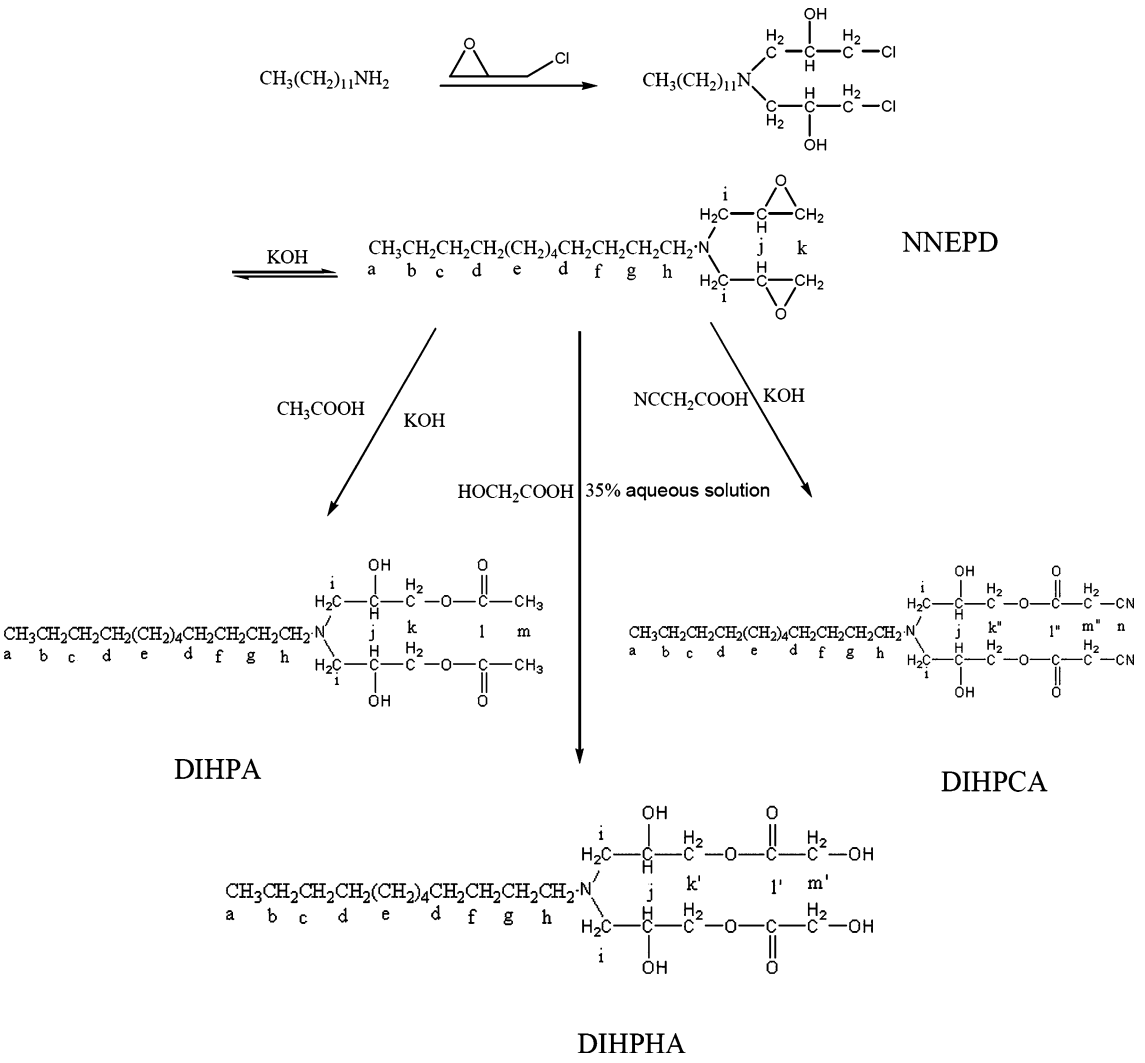

Figure 1. Preparation procedure of the alkyl bonding agents.

The aim of this study is to explore an effective method to design and select proper bonding agents which could effectively improve interfacial interactions between bonding agents and solid particles. The above founded methods have effective guiding significance for choosing proper bonding agents and improving the interfacial interactions between solid filling particles and binder matrix, whatever the composition of the propellant may be.

In this study, three types of novel bonding agents were synthesized using dodecylamine as starting material by reaction of the epoxy group from epichlorohydrin with the amino group, followed by further introduction of polar groups which can interact with AP and RDX. The reaction route is illustrated in Figure 1. The synthesized bonding agents contain both polar groups and non-polar long-chain alkyl groups. Polar groups, such as –OH, –C=O, –CN and –NH, can easily interact with the N–H, $-ClO_4^-$, or $-NO_2$ groups from the AP and RDX molecule and with –NCO groups from the binder matrix, promoting the absorptions of bonding agents to the interface of solid particles and the binder matrix. The non-polar parts of the bonding agents are distributed at the external surface of the particles and are helpful to improve the flowing properties of oxidant particles in the slurries of composite solid propellants. Once the adhesive system is solidified, long-chain alkyl groups can easily form chain entanglements and interact with the adhesive system, resulting from the combination of solid particles with adhesive agents [16–18]. Then the above three bonding agents were used as examples to explore the effective strategy for design and selection of appropriate bonding agents being useful for the propellant, going the pathway from theoretical design, via materials synthesis, study of mechanism up to practical application.

2 Experimental Section

2.1 Materials

Dodecylamine (analytical grade) was supplied by Sinopharm Chemical Reagent Co., Ltd. (China). Glycolic acid (chemical grade) was purchased from Wuhan Borui Fine Chemical Co., Ltd. Cyanoacetic acid (analytical grade) was purchased from Beijing Hengye Zhongyuan Chemical Co. Ltd. Ammonium perchlorate (AP) and hexogen (RDX) were industrial products. They were purified by passing through sieves of 200 mesh (74 μm) and 300 mesh (48 μm), respectively, and dried at 60 °C before use. All other reagents were of analytical grade, purchased from Beijing Chemical Plant (China) and used as received.

2.2 Preparation of *N,N*-di-2,3-epoxypropyl Dodecylamine (NNEPD)

Dodecylamine (9.25 g) was dissolved in ethanol (100 mL) and placed in a three neck flask with a reflux device. The solution was stirred with slow addition of epichlorohydrin (12.025 g) through a funnel. The reaction was heated in a water bath at 55 °C for 5 h and then cooled to 30 °C. After 50% KOH aqueous solution (11.2 g) was added dropwise into the flask, the mixture was stirred at 30 °C for 2 h. The products were filtered, and then ethanol and unreacted epichlorohydrin were removed by vacuum distillation. The crude product was dissolved in n-hexane (100 mL) and purified by filtration. Then n-hexane was removed by reduced pressure distillation. After drying under vacuum at 60 °C, the yellow oil-like liquid NNEPD was obtained in 92% yield. FTIR (KBr (cm^{-1})), 2924 (ν_{asCH}), 2854 (ν_{sCH}), 1461 (δ_{CH}), 1256 (ν_{asCOC}), 1115 (υ_{CN}), 917 (ν_{sCOC}), 848 (ν_{sCOC}), 723(ρ_{CH2}) ^{1}H NMR ($CDCl_3$, ppm), 2.77(H_j), 2.62(H_i), 2.43(H_k), 2.38(H_k), 2.37(H_i), 2.36(H_h), 1.39(H_g), 1.33(H_b), 1.29(H_{c-f}), 0.96(H_a). ^{13}C NMR ($CDCl_3$, ppm), 55.19(Ci), 54.95(C_h), 50.97(C_j), 44.61(C_k), 31.73(C_c), 29.44(C_e), 29.16(C_d), 26.93(C_f), 22.49(C_b), 13.92(C_a).

2.3 Preparation of Dodecylamine-*N,N*-di-2-hydroxypropylacetate (DIHPA)

KOH (0.0224 g) was dissolved in acetic acid (1.2 g) and placed in a three-neck flask with a reflux device. Afterwards, 1,4-dioxane (10 mL) and NNEPD (3.05 g) were added to the solution which was then stirred and heated in a water bath at 70 °C for 7 h. After reaction, the solvent and excess acetic acid were removed by vacuum distillation. Then the crude product was dissolved in chloroform and washed with water in a separator funnel. The funnel was allowed to stand overnight to separate the layers. The lower organic layer was vacuum distilled at 5 Pa and the product was dried in vacuo for 24 h at 5000 Pa, resulting in a dark yellow oil of DIHPA with 78% yield. FTIR (KBr (cm^{-1})), 3402 (ν_{OH}), 2924 (ν_{asCH}), 2854 (ν_{sCH}), 1741 ($\nu_{C=O}$), 1465(δ_{CH}), 1365 (δ_{OH}), 1239 (ν_{asCOC}), 1113 ($\upsilon_{CN}+\upsilon_{COH}$), 1044 ($vs_{COC}$), 722 ($\rho_{CH2}$). ^{1}H NMR ($CDCl_3$, ppm), 4.36($H_k$), 4.11($H_k$), 4.05($H_j$), 2.62($H_i$), 2.36($H_h$), 2.01($H_m$), 1.39($H_g$), 1.33($H_b$), 1.29($H_{c-f}$), 0.96($H_a$). ^{13}C NMR ($CDCl_3$, ppm), 170.3($C_l$), 68.7($C_k$), 66.2($C_j$), 56.5(Ci), 55.3($C_h$), 31.9($C_c$), 29.7($C_e$), 29.4($C_d$), 28.4($C_g$), 27.4($C_f$), 22.8($C_b$), 20.7($C_m$), 14.1($C_a$).

2.4 Preparation of Dodecylamine-*N,N*-di-2-hydroxypropyl-hydroxyacetate (DIHPHA)

Glycolic acid (17.14 g) and NNEPD (3.05 g) were placed in a 250 mL three-neck flask with a reflux device. Then the solution was stirred and heated in a water bath at 70 °C for 7 h. Acetone was added in and the unreacted glycolic acid was precipitated. Then the mixture was filtered and the solvent was removed by vacuum distillation. For further purification, the crude product was dissolved in chloroform and washed with water. The organic phase was vacuum distilled at 5 Pa and the product was dried in vacuo for 24 h at 5000 Pa to give the dark reddish-brown oil DIHPHA with 83% yield. FTIR (KBr (cm^{-1})), 3404 (ν_{OH}), 2916 (ν_{asCH}), 2854 (ν_{sCH}), 1740 ($\nu_{C=O}$), 1461 (δ_{CH}), 1370 (δ_{OH}), 1243 (ν_{asCOC}), 1109 ($\upsilon_{C-N}+\upsilon_{COH}$), 1048 ($vs_{COC}$), 848 ($\rho_{CH2}$, —$CH_2$—OH), 722 ($\rho_{CH2}$, —$(CH_2)_n$—). ^{1}H NMR ($CDCl_3$, ppm), The signals of H_a–H_k are similar to those of DIHPA, 4.49($H_{m'}$). ^{13}C NMR ($CDCl_3$, ppm), The signals of C_a–C_j are similar to those of DIHPA, 169.3($C_{l'}$), 69.0($C_{k'}$), 60.7($C_{m'}$).

2.5 Preparation of Dodecylamine-*N,N*-di-2-hydroxypropyl-cyanoacetate (DIHPCA)

Cyanoacetic acid (3.40 g) was dissolved in acetone (50 mL) and placed in a three neck flask (250 mL) with a reflux device. KOH (0.0336 g) and NNEPD (3.05 g) were added sequentially. The solution was stirred and heated in a water bath at 50 °C for 7 h. The solvent was removed by vacuum distillation. The crude product was dissolved in chloroform and washed with water in a separator funnel. The funnel was allowed to stand overnight to separate the layers. The organic layer was vacuum distilled and the product was dried in vacuo for 24 h at 5000 Pa, to yield the dark reddish-brown oil-like liquid DIHPCA. The yield was 72%. FTIR (KBr (cm^{-1})), 3370 (ν_{OH}), 2924 (ν_{asCH}), 2852 (ν_{sCH}), 2220 (ν_{CN}), 1736 ($\nu_{C=O}$), 1465 (δ_{CH}), 1357 (δ_{OH}), 1230 (ν_{asCOC}), 1113 ($\upsilon_{CN}+\upsilon_{COH}$), 1044 ($vs_{COC}$), 779 ($\rho_{CH2}$, —$CH_2$—OH), 722 ($\rho_{CH2}$). ^{1}H NMR ($CDCl_3$, ppm), The signals of H_a–H_k are similar to those of DIHPA, 3.41($H_{m''}$). ^{13}C NMR ($CDCl_3$, ppm), The signals of C_a–C_j are similar to those of DIHPA, 164.4($C_{l''}$), 116.2(C_n), 68.2($C_{k''}$), 24.6($C_{m''}$).

2.6 Molecular Dynamics Simulation

The interfacial interactions between bonding agent molecules DIHPA, DIHPHA, DIHPCA and the solid fillers, AP and RDX, were studied using the molecular dynamics simulation method by Material Studio 4.0 software, DISCOVERY modules on an IBM Blade workstation.

Three dimensional structure models were built for these three bonding molecules interacted with AP or RDX according to their structural parameters. On the basis of these models, the spatial structures of the bonding agents were simulated and optimized by the molecular mechanics method (MM). It is known that the AP crystal has space group *Pna2*, with cell parameters of $a = 0.9220$, $b = 0.7458$, $c = 0.5814$ nm and it has a density of 1.952 g cm^{-3} [19], whereas the space group of RDX is *Pbca*, with cell parameters $a = 1.3182$, $b = 1.1574$, $c = 1.0709$ nm, and $\beta = 90^{\circ}$, and it has a density of 1.816 g cm^{-3} [20]. With these parameters, the Materials Studio built the crystal structure of AP and RDX. Under the NPT ensemble, the built and geometrically optimized AP and RDX single crystal model underwent 30,000 steps of MD simulation, crystal face cutting and geometry optimization. The [120] crystal face of RDX was cut as it has the closest molecular orientation and the greatest number of molecules was enclosed by the [120] crystal plane at the same cross section [21]. In the built AP single crystal model, the [110] crystal face occupies the highest percentage of total surface area, so the [110] plane was cut.

The models for the interaction between AP or RDX and bonding agents were further built by the dynamic equilibrium approach. Using NVT ensemble under the COMPASS force field calculations [22, 23], with the force field assigned to the charge distribution pattern. The atom based pattern was used for Van Der Waals force calculations; the Ewald calculation pattern was used for Coulomb force calculations. The interaction energy $E_{interaction}$ between DIHPA, DIHPHA, DIHPCA and AP or RDX surface was calculated according to the following equation:

$$E_{interaction} = E_{total} - (E_{surface} + E_{bonding\ agent}) \quad (1)$$

Among which, E_{total} is the total energy between AP or RDX surface and bonding agents, $E_{surface}$ is the surface energy of AP or RDX after removing the bonding agent, $E_{bonding\ agent}$ is the energy of bonding agents. The more negative the $E_{interaction}$ value, the stronger the bonding capacity between the bonding agent and AP or RDX surface.

2.7 Interfacial Interaction Between the Bonding Agents and AP/RDX

The asynthesized bonding agent (0.5 g) was dissolved in ethanol (10 mL), and afterwards mixed with of AP or RDX (1 g). After being stirred at room temperature for 1 h, the mixture was filtered and the precipitate was washed with ethanol for several times. The AP or RDX particles coated by the bonding agent were dried in a water-barrier oven at 60 °C for 2 d.

The IR spectrum was obtained with a Magna-IR750 series FTIR spectrometer (Nicolet Co., USA) with an IR microscope detector. Tested samples were prepared with KBr pellets and scanned with a resolution of 3 cm^{-1} (200 scans).

XPS measurements of AP, RDX and bonding agent coated AP or RDX particles were performed with PHI 5300 X-ray photoelectron spectroscopy (Perkin–Elmer Physical Electronics Co., USA). Mg-K_{α} was used for the target (1253.6 eV) and the power was 250 W (12.5 kV at 20 mA) under a vacuum less than 10^{-6} Pa (10^{-8} Torr). The binding energies obtained herein are referenced to that from adventitious carbon, 285.0 eV and the pass energy was set at 4.5 eV. The data were processed by the XPS-PEAK special software of the test system, which bears a curve smoothing function, as well as deconvolution, X-ray satellites subtraction, background subtraction, normalization and curve fitting, etc. [24–26].

2.8 Application of Bonding Agents to HTPB Composite Propellants

The prepared bonding agents were further applied to a HTPB four-component composite solid propellant (consisting of HTPB/AP/RDX/Al), and mechanical properties of the propellant were therefore studied. The propellant had 87 wt.-% total solid content (45 wt.-% AP, 25 wt.-% RDX and 17 wt.-% Al powder), 12.85 wt.-% HTPB binder system, and 0.15 wt.-% bonding agents. The R value of propellant binder system is 0.95. The propellant slurry was kneaded and casted. The intrinsic viscosity (η) of the slurry was tested by the Brookfield R/S + SST rheometer (Brookfield Co., Ltd., USA), with a test temperature of 50 °C and a shearing rate of 1 s^{-1}. The propellant was cured at 60 °C for 7 d. The sample was sliced, cut into dumbbell-shaped pieces (according to ASTM1708-95 standard), and tested with an Instron Universal Testing Machine of Instron 1185 (Instron Co., Ltd., UK). The tests were performed at −40, 25, and 60 °C and the drawing speed was 100 mm min^{-1}. The parameters of maximum tensile strength (σ), initial modulus (E_0), elongation under maximum tensile strength (ε_m) and elongation at break of the propellant (ε_b) were obtained by the stress-strain curves.

3 Results and Discussion

3.1 Prediction of the Interfacial Interactions via Molecular Dynamics Simulations

Molecular dynamics simulation method has been widely used in predicting the performance of the binder system used for solid propellants [27–31]. In addition, molecular dynamics simulations can also be a good simulation and prediction tool for the interfacial interaction between solid filling particles, binder, and bonding agents [32–35]. In this study, molecular dynamics method was applied to simulate the interfacial interaction between the three novel synthesized bonding agents and the surface of AP and RDX.

Bonding energy plays an important role in the study of interfacial interactions. The greater the bonding energy, the stronger interfacial interaction is. Herein, the bonding ener-

Table 1. Simulated bonding energies of the three bonding agents with [110] crystal face of AP and [120] crystal face of RDX.

Filling particle	Crystal face	Bonding agent	E_{total} [kJ mol^{-1}]	$E_{surface}$ [kJ mol^{-1}]	$E_{bonding\ agent}$ [kJ mol^{-1}]	$E_{Interaction}$ [kJ mol^{-1}]
AP	[110]	DIHPA	489774.72	489782.55	1.18	−9.01
		DIHPHA	489798.20	489782.55	25.37	−9.72
		DIHPCA	489765.44	489782.55	−7.20	−9.91
RDX	[120]	DIHPA	−102057.72	−102049.13	19.97	−28.57
		DIHPHA	−101654.71	−102049.13	456.46	−62.04
		DIHPCA	−102221.91	−102049.13	−98.25	−74.54

gies of the three bonding agents with AP or RDX were systematically studied by simulations and their results are listed in Table 1.

As indicated in Table 1, there were relatively strong mutual bonding energies between [110] crystal face of AP (or [120] crystal face of RDX) and those three bonding agent molecules DIHPA, DIHPHA and DIHPCA, which suggested that those three molecules could interact with AP and RDX. As -OH from DIHPA, DIHPHA and DIHPCA molecules are easy to react with the binder matrix, those three bonding agents meet structural requirements for bonding agents and can enhance the interfacial interaction between binder matrix and AP or RDX from the theoretical modeling point of view. In addition, Table 1 indicates that for both [110] crystal face of AP or [120] crystal face of RDX the interfacial interaction energy per molar unit of the bonding agents with AP or RDX gradually increased in the sequence of DIHPA, DIHPHA and DIHPCA respectively, indicating that the interaction between AP or RDX and those three bonding agents increased in this order too.

But only when the simulating results and the experimental results were put together and their correlation was established, the predicted value of the simulating method to the interface science could just be reflected. Furthermore, interaction performance between those three bonding agents and AP or RDX was analyzed and compared by infrared spectroscopy and XPS characterization, respectively.

3.2 Comparison of the Interfacial Interactions by IR Spectroscopy

IR spectroscopy has been applied to characterize interactions between interfaces by monitoring weakening or disappearance as well as position changes of the characteristic bands. In this study, position changes of the characteristic IR bands of AP (RDX) and of AP (RDX) particles precoated with the three bonding agents described herein are compared and shown in Table 2.

When AP interacted with the bonding agents, the N–H stretching vibration band at 3286 cm^{-1} was shifted up to 6 cm^{-1} to lower wavelengths (see Table 2). The shifted bands indicate that the hydrogen bonding strength between bonding agents and the AP (N–H groups) are in the order of DIHPCA > DIHPHA > DIHPA. In the structures of these three bonding agents, there are four possible bonding groups, NR_3, OH, C=O, and –CN as main reasons to interact with AP and cause band shifting [36–38]. In the hydrogen bonding interaction formed by the C=O and –NH functions, the α-hydroxy groups in DIHPA and DIHPHA as electron donors decrease the polarity of the carbonyl groups and enhance its basic properties, thus prompting hydrogen bonding with the NH_4^+ ions. The cyan group in DIHPCA as electron withdrawing group decreases the basic properties of the carbonyl group, but the cyan groups may form hydrogen bonds with amino groups of AP too. So the infrared spectrum peak shift caused by DIHPCA is the most pronounced. After interaction with the bonding agent, the peak of AP at 1093 cm^{-1} (stretching vibration of $-ClO_4$ groups) shifted to lower wavenumbers. Presumably a small cation exchange between NH_4^+ and NHR_3^+ occurs at the surface of the AP crystal. Since the polarity of the oxygen atom in –C=O and the nitrogen atom in –CN is smaller than that of the oxygen atoms in the ClO_4 group, the latter shows the nature of an electron acceptor and the corresponding peak shifted to lower wavenumbers. Due to the co-existence of –CN and –C=O functions in DIHPCA, the red shift of DIHPCA-coated AP in this position is the most pronounced one (14 cm^{-1}), while such shift for AP interacting with DIHPHA and DIHPA has only values of 12 cm^{-1} and 9 cm^{-1}, respectively. It thus indicates that the electronic

Table 2. Position changes of the characteristic peaks for the infrared spectra of AP and RDX and precoated AP and RDX with bonding agents.

Particle	Characteristic peaks	Particle	Particle-DIHPA	Particle-DIHPHA	Particle-DIHPCA
AP	ν_{N-H}	3286	3284	3283	3280
	δ_{N-H}	1425	1424	1424	1424
	ν_{ClO4}	1093	1084	1081	1079
RDX	$\nu_{as\ NO2}$	1587, 1571, 1537	1585, 1568, 1534	1587, 1562, 1529	1587, 1562, 1522
	ν_{C-N}	1037, 924	1039, 923	1037, 922	1037, 925
	δ_{NO2}	783, 756	782, 757	784, 754	781, 756

and the induction effects between $-ClO_4$ groups and the three bonding agents are in the order of DIHPCA > DIHPHA > DIHPA. Based on the shift distances for the absorption bands of AP, the electronic effects and the induction effects between $-ClO_4$ groups with the three bonding agents must be stronger than the hydrogen bonding effects between NH_4^+ and the bonding agents.

When RDX interacted with bonding agents, the bands at 1571 and 1537 cm^{-1}, which were assigned to the stretching vibration of NO_2, shifted to lower wavenumbers. Because of the largest shift in DIHPCA-precoated RDX and the smallest shift in DIHPA-precoated RDX, it could be concluded that the interactions between RDX with the three bonding agents are in the order of DIHPCA > DIHPHA > DIHPA. The chemical shifts in the spectra can be explained from hydrogen bonding effects, electronic effects and induction effects. The only active site ($-NO_2$ group) in the RDX molecule can easily form hydrogen bonds with the hydroxyl group (–OH) of the bonding agents. DIHPHA with more available hydroxy groups has a stronger hydrogen bonding effect than DIHPA did. Presumably the –CN group is able to interact with $-NO_2$ and produces strong induction and electronic effects. Thus, DIHPCA has a stronger interaction with RDX than DIHPHA does.

3.3 Quantitative Comparison of the Interfacial Interactions by XPS Spectroscopy

XPS spectra of AP (RDX) and AP (RDX) precoated with the three bonding agents were characterized. The atom mass fraction of each element on sample surface could be obtained from the percentage of their peak areas in the XPS spectra. As nitrogen is a common element for AP, RDX and those three bonding agents, adhesive percentage R was calculated based on the molar percentage of N atoms on the crystal surface according to Ref. [39]. The R value could be calculated according to Equation (3)

$$N_R(1-R) + N_B R = N_C \quad (2)$$

$$R = \frac{N_C - N_R}{N_B - N_R} \quad (3)$$

Among which, N_R is the molar percentage of nitrogen on AP or RDX surface; N_B is the molar percentage of nitrogen for bonding agents; N_C is the molar percentage of nitrogen for bonding agents in precoated AP or RDX.

Table 3 indicates that the adhesive percentages for AP or RDX have been increased gradually from DIHPA to DIHPHA and DIHPCA, suggesting that interfacial interaction strengths between those three bonding agents and AP or RDX have been gradually increased in the same sequence.

However, it can be seen from Table 3 that there is a contamination in the test carbon source due to the limitations of the XPS test method itself, which might affect the accuracy for calculation of adhesive degrees of bonding agents on AP or RDX surface. In order to avoid the interference of carbon contamination, adhesion degrees of bonding agents on AP or RDX surface have been further explored based on the percentage of the 1s peak intensity for different N elements over the total intensity of N elements in 1s photoelectron spectra obtained by a narrow scan. The formula for calculation is [40,41]:

$$R = \frac{A_{N1s-B}}{A_{N1s-C}} \quad (4)$$

Among which, A_{N1s-B} refers to the peak area of >N- in a narrow scan; while A_{N1s-C} refers to N1s total peak area in a narrow scan.

The data were processed by the XPS-PEAK software of the test system which employs a least square approximation method, with the peak position and FWHM as adjustable parameter and the peak position of the same bond kept as close as possible. The fitted N1s spectra of AP and AP precoated with the three bonding agents, N1s spectra of RDX and RDX precoated with the three bonding agents are all shown in Figure 2. The adhesion degrees of different bonding agents on the surface of RDX were calculated according to equation (3) and summarized in Table 4.

In the pure AP crystal, the emission peak for N1s of $-NH_4^+$ occurred at 401.99 eV (shown in Table 4). But after interaction with bonding agents, the electron density of $-NH_4^+$ decreased and the emission peak shifted to around 402.5 eV due to hydrogen bonding between NR_3, –OH, –C=O, and –CN. The peak at around 400 eV is ascribed to the tertiary nitrogen in bonding agents, as opposed to

Table 3. XPS results and adhesive degrees of AP and RDX and precoated AP and RDX with bonding agents.

Sample	C [%]	O [%]	N [%]	Cl [%]	R [%]
AP	39.20	30.25	25.29	5.26	0
AP-DIHPA	39.60	30.09	24.94	5.37	1.59
AP-DIHPHA	40.20	29.31	24.81	5.26	2.17
AP-DIHPCA	40.47	29.28	24.91	5.34	2.36
RDX	39.24	33.04	27.72	–	0
RDX-DIHPA	40.40	32.40	27.20	–	2.12
RDX-DIHPHA	42.25	31.00	26.75	–	3.95
RDX-DIHPCA	41.96	31.11	26.93	–	4.23

Table 4. Specification and contents of sample N1s spectra.

Sample	Functionality of N atom	Binding energy [eV]	Content [%]	*R* [%]
AP	$-NH_4^+$	401.99	100	0
AP-DIHPA	$-NH_4^+$	402.43	81.85	18.15
	>N–	400.41	18.15	
AP-DIHPHA	$-NH_4^+$	402.49	63.67	36.33
	>N–	399.90	36.33	
AP-DIHPCA	$-NH_4^+$	402.55	58.11	41.89
	>N–	400.06	37.29	
	–CN	399.62	4.60	
RDX	$-NO_2$	407.88	49.9	0
	>N–NO_2	402.28	50.1	
RDX-DIHPA	$-NO_2$	407.83	34.82	36.65
	>N–NO_2	402.16	28.53	
	>N	400.13	36.65	
RDX-DIHPHA	$-NO_2$	408.25	21.80	46.97
	>N–NO_2	401.90	31.23	
	>N	400.18	46.97	
RDX-DIHPCA	$-NO_2$	408.08	21.30	51.00
	>N–NO_2	401.92	27.70	
	>N	400.58	22.32	
	–CN	399.23	28.68	

Note: During the process of calculating the actual binding energies, the charging effects for carbon contamination were subtracted according to Ref. [33]. The binding energies listed in the Table were all modified by subtracting the charging effect. At the experimental conditions, the charge electric displacement caused by carbon pollution was 0.70 eV for AP and 2.49 eV for RDX.

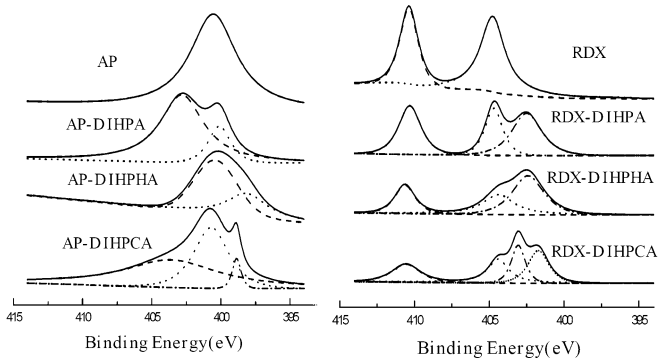

Figure 2. Fitting curves of the XPS N1s spectra for neat AP and RDX solid particles and precoated particles with the three bonding agents.

DIHPA, DIHPHA, and DIHPCA. The latter has a –CN absorption peak occurring at 399.62 eV. Based on the data in Table 4, the adhesion degrees of DIHPA, DIHPHA and DIHPCA with AP are 18.15, 36.33, and 41.89%, respectively. This also indicates that the interaction strength between the three bonding agents and AP are in the order of DIHPCA > DIHPHA > DIHPA.

Since the electron withdrawing effects of oxygen atoms in the $-NO_2$ group are higher than those of oxygen atoms in –C=O groups and nitrogen atoms in –CN, the $-NO_2$ group with the more positively charged nitrogen acts as an electron acceptor. After interaction of RDX with bonding agents, the electron density of $-NO_2$ on the outer shell increased and the emission peaks for N1s of $-NO_2$ and >N–NO_2 in RDX moved to the direction of lower bond energies. At the same time, the emission peak for N1s of >N and –CN in the sample appeared. From Table 4, it could be concluded that interactions of the bonding agents with RDX increased in the range DIHPA < DIHPHA < DIHPCA. The corresponding *R* values are 36.65, 46.97, and 51.00%, respectively.

Through the above IR and XPS spectroscopic studies, the interface interactions between the bonding agents and the filling particles could be quantitatively evaluated and compared. The results are in well agreement.

3.4 Practical Application of the Bonding Agents in HTPB Composite Propellants

The prepared bonding agents were also applied to HTPB four-group composite propellants. The mechanical properties of the propellants were studied at high, normal and low temperatures, and compared with the control samples without bonding agents. When the three bonding agents were added to the HTPB four-group propellant, maximum tensile strength (σ), initial modulus (E_0), elongation under maximum tensile strength (ε_m) and elongation at breaking point of the propellant (ε_b) at different temperatures could be significantly improved (see Table 5), if compared to the control samples. The adhesion index (Φ) of the propellants after adding the bonding agents was lower than that of the control samples, which indicates that addition of bonding agents effectively changed the interfacial interactions between the solid components (AP, RDX, etc.) and binder matrix. The values for tensile strength and elongation were

Table 5. Effects of the three bonding agents on the mechanical properties of HTPB-based composite propellants.

		Blank	DIHPA	DIHPHA	DIHPCA
25 °C	σ [MPa]	0.42	0.63	0.86	1.08
	E_0 [MPa]	3.86	4.21	4.43	4.75
	ε_m [%]	22.7	32.1	39.7	46.2
	ε_b [%]	33.0	43.6	44.8	51.7
	Φ	1.454	1.358	1.128	1.119
60 °C	σ [MPa]	0.36	0.57	0.76	0.83
	E_0 [MPa]	2.96	3.29	3.61	3.67
	ε_m [%]	25.7	36.4	43.1	49.7
	ε_b [%]	36.0	44.5	52.3	53.4
	Φ	1.401	1.223	1.213	1.074
−40 °C	σ [MPa]	1.55	1.73	1.79	1.91
	E_0 [MPa]	11.91	12.55	13.97	13.29
	ε_m [%]	13.7	20.3	26.2	36.1
	ε_b [%]	27.0	36.1	42.9	44.8
	Φ	1.971	1.778	1.637	1.241
η [Pa s]		657.5	611.9	597.8	632.9

$\Phi = \varepsilon_b/\varepsilon_m$ indicates the adhesion index between filling particles and binder matrix.

simultaneously enhanced, which confirms the efficiency of the bonding agents [42,43]. The σ, E_0, ε_m, and ε_b values could be continuously improved for DIHPCA > DIHPHA > DIHPA modified energetic particles. The Φ value was gradually reduced and close to 1 in accordance with the trend of DIHPA, DIHPHA, and DIHPCA modification. The position of maximum strain is very close to that of material failure, indicating that the three bonding agents as "molecular bridges" gradually improved the adhesions between filler particles and binder. These results confirmed our conclusions from the infrared spectrum and XPS characterizations. Additionally the intrinsic viscosities of the propellant slurries with bonding agents were all decreased compared to the control slurry. The above results demonstrate that the bonding agents with the long dodecyl chain are helpful to improve the flowing properties of oxidant particles in the slurries of composite solid propellants.

4 Conclusions

Preparation and property studies of three novel alkyl bonding agents, DIHPA, DIHPHA and DIHPCA were presented. The properties of interfacial interaction of the bonding agents with AP or RDX were forecasted through the molecular dynamics simulation. The interfacial interactions of bonding agents with AP or RDX were investigated by IR and XPS spectroscopy. The actual application effects of the bonding agents were tested by the HTPB four-group propellant.

The laboratory observation tests of these bonding agents used in composite propellants were in well agreement with the theoretical and spectroscopic results. All observations indicated that the pathway from theoretical design, materials synthesis, mechanism study, to practical application is an effective strategy to improve the interfacial interaction between the surface of the solid particles and bonding agents, which is a complicated scenario and thus hard to be studied.

As there is little systematic method to design and choose the proper bonding agent that could really improve the interfacial interactions between the solid filling particles and binder matrix in the previous literature. The above established methods have effective guiding significance to choose the proper bonding agent and improve the interfacial interactions between the solid filling particles and binder matrix in most propellant compositions.

List of Abbreviations and Symbols

DIHPA	Dodecylamine-*N*,*N*-di-2-hydroxypropyl-acetate
DIHPHA	Dodecylamine-*N*,*N*-di-2-hydroxypropyl-hydroxy-acetate
DIHPCA	Dodecylamine-*N*,*N*-di-2-hydroxypropyl-cyano-acetate
COMPASS	Condensed-phase Optimized Molecular Potentials for Atomistic Simulation Studies
FWHM	Full width at half maximum
η	Intrinsic viscosity
σ	Tensile strength
E_0	Initial modulus
ε_m	Elongation under maximum tensile strength
ε_b	Elongation at breaking point of the propellant
Φ	Adhesion index
$E_{interaction}$	The interaction energy
E_{total}	The total energy between AP or RDX surface and bonding agents
$E_{surface}$	The surface energy of AP or RDX after removing the bonding agent,
$E_{bonding\ agent}$	The energy of bonding agents.
HTPB	Hydroxyl-terminated polybutadiene

R	Adhesive percentage
N_R	Molar percentage of nitrogen on AP or RDX surface
N_B	Molar percentage of nitrogen for bonding agents
N_C	Molar percentage of nitrogen for bonding agents in precoated AP or RDX
NNEPD	*N*,*N*-di-2,3-epoxypropyl dodecylamine
NVT	Canonical ensemble with certain particle number (N), volume(V) and temperature (T)
XPS	X-ray photoelectron spectroscopy#

Acknowledgments

This work was supported by the National Natural Science Foundation of China (No. 51073025).

References

[1] N. Niehaus, O. Greeb, Optimization of Propellant Binders – Part Two: Macroscopic Investigation of the Mechanical Properties of Polymers, *Propellants Explos. Pyrotech.* **2004**, *29*, 333.
[2] G. S. Tussiwand, V. E. Saouma, R. Terzenbach, L. T. De Luca, Fracture Mechanics of Composite Solid Rocket Propellant Grains: Material Testing, *J. Propul. Power* **2009**, *25*, 60.
[3] P. H. Geubelle, H. M. Inglis, J. D. Kramer, J. J. Patel, N. C. Kumar, H. Tan, Multiscale Modeling of Dewetting Damage in Highly Filled Particulate Composites, *AIP Conf. Proc.* **2008**, 973, 196.
[4] W. Zhang, X. Z. Fan, H. J. Wei, J. Z. Li, Application of Nitramines Coated with Nitrocellulose in Minimum Signature Isocyanate-Cured Propellants, *Propellants Explos. Pyrotech.* **2008**, *33*, 279.
[5] J. C. Li, Q. J. Jiao, H. Ren, D. Li, Preparation of NC-BA-RDX Coating Ball Particles by Means of Layer-to-Layer Assembly Technique, *J. Solid Rocket Technol.* **2008**, *31*, 247.
[6] T. F. Nihal, U. B. Zühtü, The Effect of Ammonium Nitrate, Coarse/Fine Ammonium Nitrate Ratio, Plasticizer, Bonding Agent, and Fe_2O_3 Content on Ballistic and Mechanical Properties of Hydroxyl Terminated Polybutadiene Based Composite Propellants Containing 20% AP, *J. ASTM Int.* **2005**, *2*, 233.
[7] A. A. Ali, J. W. Zhang, G. B. Cai, Investigation of the Role of Aziridine Bonding Agents on the Aging of the Composite Solid Rocket Propellant (CSRP), *J. Aerosp. Power* **2008**, *23*, 2101.
[8] J. Sciamareli, M. F. K. Takahashi, J. M. Teixeira, Solid Polyurethane-Based Composite Propellant: I – Influence of the Bonding Agent, *Quim. Nova.* **2002**, *25*, 107.
[9] X. H. Zhang, F. Q. Zhao, H. M. Tan, Improving Mechanical Property of CMDB Propellant Containing Nitramine with Bonding Agent, *Chin. J. Explos. Propellants* **2005**, *28*, 1.
[10] F. Q. Zhao, W. G. Shan, S. W. Li, Review on Silane Coupling Agents Used in Solid Rocket Motor Charges and Their Action Mechanism, *Energ. Mater.* **1998**, *6*, 37.
[11] E. Landsem, T. L. Jensen, F. K. Hansen, E. Unneberg, T. E. Kristensen, Neutral Polymeric Bonding Agents (NPBA) and Their Use in Smokeless Composite Rocket Propellants Based on HMX-GAP-BuNENA, *Propellants Explos. Pyrotech.* **2012**, *37*, 581.
[12] B. S. Min, Y. C. Park, J. C. Yoo, A Study on the Triazole Cross-linked Polymeric Binder Based on Glycidyl Azide Polymer and Dipolarophile Curing Agents, *Propellants Explos. Pyrotech.* **2012**, *37*, 59.
[13] D. C. Pires, A. M. Kawamoto, J. Sciamareli, E. C. Mattos, M. F. Diniz, R. C. L. Dutra, Synthesis and Characterization by Infrared Spectroscopy of Hydantoin-Based Bonding Agents, Used in Composite Propellants, *J. Aerosp. Technol. Manage.* **2009**, *1*, 55.
[14] H. X. Tang, X. L. Liu, Q. Wu, Action Mechanism of Special Functional Agents in Composite Solid Propellant (IV) – Processability/Mechanical Properties, *J. Solid Rocket Technol.* **2004**, *27*, 193.
[15] Y. Wang, G. Qiu, Thermal Behavior of Bonding Agent 1,1-(1,3-Phenylenedicarbonyl) Bis-2-methyl-aziridine, *J. Propul. Technol.* **2001**, *22*, 258.
[16] L. Du, J. W. Xiao, R. K. Yin, Low Temperature Mechanical Properties of High-Burning Rate HTPB/IPDI Propellants (II) Design and Application of Surfactants, *J. Propul. Technol.* **2002**, *23*, 245.
[17] H. X. Li, H. X. Tang, J. R. Deng, M. C. Zhou, Mechanism of PB Aids Added in Nitrate Plasticized Propellants, *J. Propul. Technol.* **2002**, *23*, 164.
[18] H. X. Tang, X. L. Liu, Q. Wu, Action Mechanism of Special Functional Agents in Composite Solid Propellants (II) HTPB/Al System, *J. Solid Rocket Technol.* **2002**, *25*, 41.
[19] J. G. Zhang, T. L. Zhang, L. Yang, K. B. Yu, A Study of Crystal Structure and Explosive Properties of Ammonium Perchlorate, *Chin. J. Explos. Propellants* **2002**, *25*, 33.
[20] R. G. Stacer, D. M. Husband, Molecular Structure of the Ideal Solid Propellant Binder, *Propellants Explos. Pyrotech.* **1991**, *16*, 167.
[21] J. H. Ter Horst, R. M. Geertman, G. M. van Rosmalen, The Effect of Solvent on Crystal Morphology, *J. Cryst. Growth* **2001**, *230*, 277.
[22] J. J. Xiao, G. Y. Fang, G. F. Ji, H. M. Xiao, Simulation Investigations in the Binding Energy and Mechanical Properties of HMX-Based Polymer-Bonded Explosives, *Chin. Sci. Bull.* **2005**, *50*, 21.
[23] R. H. Gee, A. Maiti, S. Bastea, L. E. Fried, Molecular Dynamics Investigation of Adhesion Between TATB Surfaces and Amorphous Fluoropolymers, *Macromolecules* **2007**, *40,* 3422.
[24] G. X. Zhao, S. J. Jia, S. Qian, D. M. Feng, State Analysis of the Surface Elements of PAN-Based Carbon Film during the Formation, *New Carbon Mater.* **1997**, *4*, 1.
[25] Y. Qian, P. Wei, P. K. Jiang, J. W. Hao, J. X. Du, Preparation of Hybrid Phosphamide Containing Polysilsesquioxane and Its Effect on Flame Retardancy and Mechanical Properties of Polypropylene Composites, *Composites B* **2013**, *45*, 1541.
[26] Y. Zhou, J. W. Hao, G. S. Liu, J. X. Du, Influencing Mechanism of Transition Metal Oxide on Thermal Decomposition of Ammonium Polyphosphate, *Chin. J. Inorg. Chem.* **2013**, *29*, 1115.
[27] H. L. Xiao, Q. Z. Feng, H. J. Xue, Molecular Dynamics simulation on Miscibility of Trans-1,4,5,8-tetranitro-1,4,5,8-tetraazadecalin (TNAD) with Some Propellants, *J. Mol. Model.* **2013**, *19*, 2391.
[28] Y. D. Luo, J. H. Chen, C. I. Huang, W. Y. Chiu, Molecular Dynamics Study of TiO_2/Poly(Acrylic Acid-Comethyl Methacrylate) and Fe_3O_4/Polystyrene Composite Latex Particles Prepared by Heterocoagulation, *J Appl. Polym. Sci.* **2010**, *116*, 2275.
[29] N. R. Tummala, L. Shi, A. Striolo, Molecular Dynamics Simulations of Surfactants at the Silica-Water Interface: Anionic vs. Nonionic Headgroups, *J. Colloid Interf. Sci.* **2011**, *362*, 135.
[30] C. D. Wu, T. H. Fang, J. F. Lin, Effect of Chain Length of Self-Assembled Monolayers in dip-pen Nanolithography Using Molecular Dynamics Simulations, *J. Colloid Interf. Sci.* **2011**, *361*, 316.
[31] J. Pietrasik, M. Gaca, M. Zaborski, L. Okrasa, G. Boiteux, O. Gain, Studies of Molecular Dynamics of Carboxylated Acryloni-

trile-Butadiene Rubber Composites Containing In situ Synthesized Silica Particles, *Eur. Polym. J.* **2009**, *45*, 3317.

[32] G. C. Li, Y. G. Xing, Y. F. Wang, A. M. Pang, X. Guo, G. Tang, Micromechanical Method of the Effective Modulus Estimation for the Composite Propellant, *J. Propul. Technol.* **2007**, *28*, 441.

[33] J. J. Xiao, L. Zhao, W. Zhu, J. Chen, G. F. Ji, F. Zhao, Molecular Dynamics Study on the Relationships of Modeling, Structural and Energy Properties with Sensitivity for RDX-Based PBXs, *Sci. Chin. Chem.* **2012**, *55*, 2587.

[34] W. M. Wu, W. Zhang, M. B. Chen, H. F. Qiang, L. W. Shi, Theoretical Investigation of the Bond Dissociation of Hydroxyl Terminated Polybutadiene Binder and Effect on Mechanical Properties, *Acta Chim. Sin. (Engl. Ed.)* **2012**, *70*, 1145.

[35] Y. C. Yang, D. M. Jiao, H. F. Qiang, G. Wang, Molecular Simulation of Solubility Parameter for HTPB Solid Propellants, *Chin. J. Energ. Mater.* **2008**, *16*, 191.

[36] B. F. Pan, Y. J. Luo, H. M. Tan, Study on Interaction Between CL-20 and Dendritic Bonding Agent, *Chin. J. Energ. Mater.* **2004**, *12*, 199.

[37] B. Zhang, Y. J. Luo, H. M. Tan, Interactional Mechanism of the Interface between CL-20 and Some Bonding Agents, *Chin. J. Explos. Propellants* **2005**, *28*, 23.

[38] J. C. Li, Q. J. Jiao, H. Ren, L. X. Wang, W. D. Zhao, RDX coated with hydantoin/triazines composite bonding agent, *Chin. J. Energ. Mater.* **2008**, *16*, 56.

[39] Y. Yang, Y. J. Luo, Y. B. Jiu, M. N. Du, Y. Lv, Z. Ge, Influence of CL-20 Coated with Thermoplastic Polyurethane Elastomers (TPU) on Mechanical Properties of NEPE Propellant, *J. Solid Rocket Technol.* **2008**, *31*, 358.

[40] H. B. Yang, W. Fu, L. X. Chang, M. H. Li, H. Bala, Q. J. Yu, Preparation and Characteristics of Core-Shell Structure Nickel/Silica Nanoparticles, *Colloids Surf. A* **2005**, *262*, 71.

[41] L. Shi, *Preparation and Properties Study on the Alkyl Bonding Agents*, M. S. Thesis, Beijing Institute of Technology, Beijing, P. R. China, **2008**.

[42] R. X. Cui, W. Zhang, L. Chen, Synthesis and Application of Borate Bonding Agents for AP/RDX/Al/HTPB Propellant, *J. Solid Rocket Technol.* **2012**, *35*, 374.

[43] L. L. Meng, W. X. Xie, H. J. Yu, X. H. Zhang, W. Zhang, Y. D. Chen, Influence of Bonding Agents on Mechanical Properties of Nitrate Plasticized BAMO-THF Propellants, *Chem. Propellants Polym. Mater.* **2011**, *9*, 65.

Received: December 2, 2013
Revised: April 16, 2014
Published online: October 2, 2014

